

Correlations of the upper branch of 1d harmonically trapped two-component Fermi gases

Seyed Ebrahim Gharashi¹ and D. Blume^{1,2}

¹*Department of Physics and Astronomy, Washington State University, Pullman, Washington 99164-2814, USA*

²*ITAMP, Harvard-Smithsonian Center for Astrophysics,
60 Garden Street, Cambridge, Massachusetts 02138, USA*

(Dated: April 13, 2018)

We present highly-accurate energy spectra and eigen functions of small 1d harmonically trapped two-component Fermi gases with interspecies δ -function interactions, and analyze the correlations of the so-called upper branch (i.e., the branch that describes a repulsive Fermi gas consisting of atoms but no molecules) for positive and negative coupling constants. Changes of the two-body correlations as a function of the interspecies coupling strength reflect the competition of the interspecies interaction and the effective repulsion due to the Pauli exclusion principle, and are interpreted as a few-body analog of a transition from a non-magnetic to a magnetic phase. Moreover, we show that the eigenstate ψ_{adia} of the infinitely strongly-interacting system with $|n_1 + n_2| > 2$ and $|n_1 - n_2| < n$ (n_1 and n_2 denote the number of fermions of components 1 and 2, respectively), which is reached experimentally by adiabatically changing the system parameters, does not, as previously proposed, coincide with the wave function ψ_G obtained by applying a generalized Fermi-Fermi mapping function to the eigen function of the non-interacting single-component Fermi gas.

PACS numbers:

1d systems serve as powerful models whose study provides insights into fundamental phenomena such as gas dynamics, electron transport, Cooper pairing and superconductivity [1–4]. In the special case where the interactions between the particles are modeled by zero-range δ -functions, the quantum mechanical problem becomes integrable. The integrability has many important consequences. For example, 1d systems with δ -function interactions can, if external forces are absent and periodic boundary conditions are imposed, be solved via the Bethe ansatz [5]. Another consequence of the integrability is the fact that a single-component Bose gas with infinitely strong δ -function interactions behaves like an impenetrable Bose gas, referred to as Tonks-Girardeau gas [6–9]. The corresponding bosonic wave function has similarities with that of a gas of non-interacting (NI) fermions; in fact, the bosonic wave function can be mapped to the fermionic wave function via a Bose-Fermi mapping [7, 10–12]. This Bose-Fermi duality has wide ranging applications. In studies of lattice Hamiltonian, e.g., it implies that bosonic creation and annihilation operators can be mapped to fermionic ones, and vice versa.

Given the success of the Bose-Fermi duality for single-component Bose and Fermi gases, it is intriguing to ask whether analogous dualities exist for trapped multi-component gases with interspecies δ -function interactions with coupling strength g . This question is not only of fundamental interest but directly relevant to ongoing cold atom experiments on effectively 1d two-component Fermi gases [13, 14]. Indeed, a generalized Fermi-Fermi mapping was recently formulated for harmonically trapped two-component Fermi gases with infinitely large interspecies δ -function interactions. The generalized Fermi-Fermi mapping [15] states that an eigenstate ψ_G of the trapped two-component Fermi gas with $|g| \rightarrow \infty$ can be

obtained, for any n ($n = n_1 + n_2$), by applying a mapping function M_{FF} to the eigen function ψ_{ideal} of the NI harmonically trapped one-component Fermi gas, i.e., $\psi_G = M_{\text{FF}}\psi_{\text{ideal}}$. This Letter shows that the states ψ_G , constructed according to the generalized Fermi-Fermi mapping, do in general not agree with the eigenstates ψ_{adia} of the two-component Fermi gas, which emerge by adiabatically evolving the system Hamiltonian from the NI to the infinitely strongly-interacting regime. For $n > 2$ and $|n_1 - n_2| < n$, the eigenenergies for states with a given parity for $|g| \rightarrow \infty$ are degenerate [16], thereby explaining how ψ_G can be an eigenstate but not coincide with any of the states that are reached by performing an adiabatic sweep.

We also calculate the pair correlation functions of the upper branch of the $(n_1, n_2) = (2, 1)$, $(3, 1)$ and $(2, 2)$ systems. The energy of the upper branch, which corresponds to a metastable repulsive atomic gas, lies above that of the NI system, and is populated by starting from the NI regime and turning on repulsive interspecies interactions. The changes of the structural correlations as the coupling constant is changed from small and positive, to infinitely large, to small and negative reflect the competition between the interspecies interactions and the Pauli pressure introduced by the anti-symmetry requirement of the wave function under the exchange of identical fermions. The expectation value of the intraspecies distance coordinate exhibits a maximum at g_c . For $-1/g \lesssim -1/g_c$, the interactions are “weaker” than the Pauli exclusion principle and the expectation value of the intra- and interspecies distances increase with increasing $-1/g$. For $-1/g \gtrsim -1/g_c$, in contrast, the interactions become so strong that the system prefers to reduce the distance between like particles with increasing $-1/g$. These structural changes are interpreted as constituting a smooth

few-body analog of the transition from a non-magnetic to a magnetic phase. The question whether 3d atomic two-component Fermi gases undergo, if “driven up” the upper branch, a transition from a paramagnetic to an itinerant ferromagnetic phase, as described by the Stoner model [17], has recently been studied extensively experimentally and theoretically for 3d two-component Fermi gases [18–25].

We consider n 1d fermions with mass m and position coordinates z_j . Assuming interspecies δ -function interactions with coupling strength g , the Hamiltonian reads

$$H = \sum_{j=1}^n \left(\frac{-\hbar^2}{2m} \frac{\partial^2}{\partial z_j^2} + \frac{1}{2} m \omega^2 z_j^2 \right) + \sum_{j=1}^{n_1} \sum_{k=n_1+1}^n g \delta(z_{jk}), \quad (1)$$

where ω denotes the angular trapping frequency and $z_{jk} = z_j - z_k$. Throughout, we assume $n_1 \geq n_2$. The solutions for the $(n_1, n_2) = (1, 1)$ system are known semi-analytically for all g [26]. For $n > 2$, in contrast, the eigenenergies and eigenstates are, in general, not known analytically and we resort to a numerical approach. To solve the time-independent Schrödinger equation for the Hamiltonian H , we separate the center of mass motion and expand the Green’s function for the relative coordinates in terms of harmonic oscillator states. For the $(2, 1)$ system, the approach has been detailed in Ref. [27]. For the $(3, 1)$ and $(2, 2)$ systems, we generalize the formalism of Refs. [27–31]. Throughout, we assume that the center of mass wave function is in the ground state and label the relative eigenstates by the relative parity Π^{rel} ($\Pi^{\text{rel}} = \pm 1$). Our calculations yield highly-accurate energy spectra and wave functions as a function of g . For $g = 0$, the ground state of the $(2, 1)$ has $\Pi^{\text{rel}} = -1$, that of the $(3, 1)$ system has $\Pi^{\text{rel}} = -1$, and that of the $(2, 2)$ system has $\Pi^{\text{rel}} = +1$; in the following, we restrict ourselves to these subspaces.

Figure 1 shows the relative eigenenergies of the $(2, 1)$, $(3, 1)$ and $(2, 2)$ systems as a function of $-E_{\text{ho}} a_{\text{ho}}/g$, where E_{ho} and a_{ho} denote respectively the harmonic oscillator energy and length, $E_{\text{ho}} = \hbar\omega$ and $a_{\text{ho}} = \sqrt{\hbar/(m\omega)}$. For $g \rightarrow 0^+$ (far left of the graphs), the eigenenergies approach the NI limit. As g increases, the eigenenergies increase, reflecting the repulsive character of the δ -function interactions. In this work, we are primarily interested in the upper branches shown by thick solid lines in Fig. 1 [31]. For $1/|g| = 0$, the relative energy of the upper branch is expected, assuming that some kind of generalized fermionization takes place, to equal $(n^2 - 1)E_{\text{ho}}/2$. Our numerical energies agree with this expectation to better than 0.0001%, 0.005% and 0.02% for the $(2, 1)$, $(3, 1)$ and $(2, 2)$ systems, respectively [32]. For negative g , the spectrum changes notably. In this regime, the upper branch corresponds to a highly excited state of the model Hamiltonian. In addition to states whose energies change fairly gradually with $-1/g$, there exists a set of “diving states”, reflecting the fact that the 1d δ -function potential with negative g supports a two-body bound state. The fact that the two-body binding energy

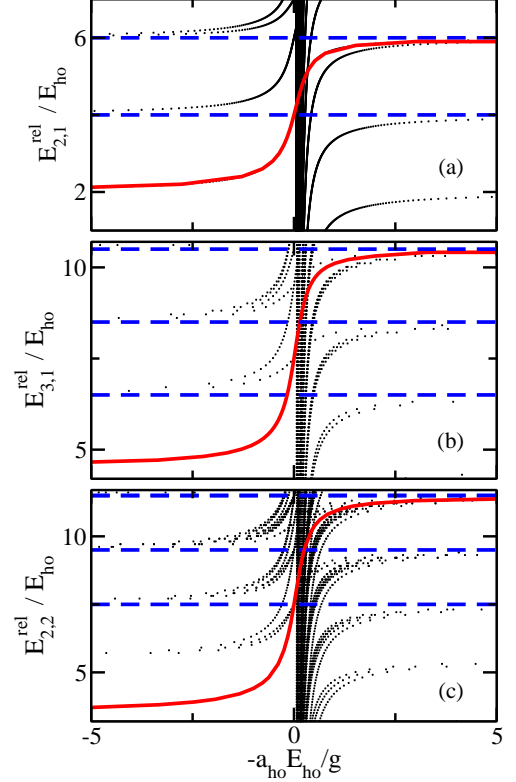


FIG. 1: (Color online) Relative energies for the (a) $(2, 1)$ system with $\Pi^{\text{rel}} = -1$, (b) $(3, 1)$ system with $\Pi^{\text{rel}} = -1$, and (c) $(2, 2)$ system with $\Pi^{\text{rel}} = +1$ as a function of $-1/g$. The dashed lines show the eigenenergies corresponding to states that are not affected by the interspecies interactions. The thick solid lines show the upper branch.

goes to $-\infty$ for $g \rightarrow -\infty$ leads to the accumulation of diving states in Fig. 1 for small positive $-a_{\text{ho}} E_{\text{ho}}/g$. For positive g , the upper branch was mapped out in Ref. [34]. For negative g , the upper branch has been mapped out for the $(2, 1)$ system [35] but not $n > 3$.

We now discuss the $(2, 1)$ eigenstate of the upper branch with $1/|g| = 0$. The energy of the upper branch of the $(2, 1)$ system with $1/|g| = 0$ is degenerate with the energy of a state that is not affected by the δ -function interactions [see lowest dashed line in Fig. 1(a)]. The two degenerate eigenstates $\psi_{\text{adia},1}^{|g|=\infty}$ and $\psi_{\text{adia},2}^{|g|=\infty}$ [corresponding to the solid and lowest dashed lines in Fig. 1(a)] are, including the center-of-mass contribution, given by [33]

$$\psi_{\text{adia},1}^{|g|=\infty} = \frac{a_{\text{ho}}^{-9/2}}{2\sqrt{3}\pi^{3/4}} z_{12}(z_{13}z_{23} - 3|z_{13}||z_{23}|)f(z_1, z_2, z_3)(2)$$

with $f(z_1, \dots, z_n) = e^{-\sum_{j=1}^n z_j^2/(2a_{\text{ho}}^2)}$ and $\psi_{\text{adia},2}^{|g|=\infty} = \psi_{\text{ideal},0}(z_1, z_2, z_3)$, where

$$\psi_{\text{ideal},0}(z_1, z_2, z_3) = \frac{\sqrt{2}a_{\text{ho}}^{-9/2}}{\sqrt{3}\pi^{3/4}} z_{12}z_{13}z_{23}f(z_1, z_2, z_3). \quad (3)$$

Since the eigenstate $\psi_{\text{adia},1}^{|g|=\infty}$ changes smoothly when the system Hamiltonian is changed adiabatically ($\psi_{\text{adia},2}^{|g|=\infty}$ is unchanged), we refer to these states as “adiabatic eigenstates”. According to the generalized Fermi-Fermi mapping [15], $\psi_{\text{adia},1}^{|g|=\infty}$ should coincide with the state $\psi_{G,0}$, which is obtained by applying the spin-dependent mapping function M_{FF} ($\sigma_j = \uparrow$ for $j = 1, \dots, n_1$ and $\sigma_j = \downarrow$ for $j = n_1 + 1, \dots, n$) [15],

$$M_{\text{FF}} = \prod_{1 \leq j < k \leq n} [(\delta_{\sigma_j \uparrow} \delta_{\sigma_k \downarrow} - \delta_{\sigma_k \downarrow} \delta_{\sigma_j \uparrow}) \text{sgn}(z_{jk}) + \delta_{\sigma_j \uparrow} \delta_{\sigma_k \uparrow} + \delta_{\sigma_j \downarrow} \delta_{\sigma_k \downarrow}], \quad (4)$$

to the energetically lowest lying eigenstate $\psi_{\text{ideal},0}$ of the trapped NI single-component Fermi gas. We find, however, that this is not the case. Instead, we find that $\psi_{G,0}$ has non-unit overlap with $\psi_{\text{adia},1}^{|g|=\infty}$ and $\psi_{\text{adia},2}^{|g|=\infty}$, i.e., $|\langle \psi_{\text{adia},j}^{|g|=\infty} | \psi_{G,0} \rangle|^2 = 8/9$ and $1/9$ for $j = 1$ and 2 , respectively.

The (3,1) and (2,2) systems with $1/|g| = 0$ support respectively two and four degenerate states with $E^{\text{rel}} = 15E_{\text{ho}}/2$. For the (3,1) system, both states are affected by the δ -function interactions. For the (2,2) system, three of the four states are affected by the δ -function interactions. We find $|\langle \psi_{\text{adia},1}^{|g|=\infty} | \psi_{G,0} \rangle|^2 = 4/5$ and $0.865(7)$ for the (3,1) and (2,2) systems, respectively [33]. This indicates that $\psi_{G,0}$ is, for $n > 2$ and $n_1 - n_2 > 0$, a linear combination of the $\psi_{\text{adia},j}^{|g|=\infty}$ ($j = 1, 2, \dots$). Thus, starting in the energetically lowest lying eigenstate of the NI system, an adiabatic sweep from $g = 0^+$ to $g \rightarrow \infty$ does not only lead to population of the “fermionized state” $\psi_{G,0}$ but also to population of one or more additional states that are orthogonal to $\psi_{G,0}$.

Figures 2(a) and 2(b) show contour plots of the wave functions $\psi_{\text{adia},1}^{|g|=\infty}$ and $\psi_{G,0}$, respectively, for the (2,1) system with $1/|g| = 0$ as functions of the up-up distance coordinate z_{12} and the Jacobi coordinate $z_{12,3}$, $z_{12,3} = (z_{13} + z_{23})/\sqrt{3}$. The most striking feature is that $\psi_{G,0}$ appears to have a higher “symmetry” than $\psi_{\text{adia},1}^{|g|=\infty}$. This is highlighted in the eigen function cuts shown in Fig. 2(c). The absolute value of the slope of the wave function $\psi_{G,0}$ near the nodes at $z_{12} = \pm\sqrt{3}a_{\text{ho}}$, corresponding to $z_{13} = 0$ and $z_{23} = 0$, is the same to the left and right of the node [see solid line in Fig. 2(c)]. Mapping $\psi_{G,0}$ so that it is anti-symmetric with respect to $z_{13} = 0$ and $z_{23} = 0$ and describing the interspecies interactions through δ' -functions in first-order perturbation theory, we find $E/E_{\text{ho}} \approx 9/2 + cE_{\text{ho}}a_{\text{ho}}/(g\sqrt{2\pi})$ with $c = 9$. From our numerical results, in contrast, we extract $c = 81/8$. This discrepancy highlights that the generalized Fermi-Fermi mapping cannot, in general, be utilized within a perturbative framework. Figure 2(c) shows that the wave function $\psi_{\text{adia},0}$ is neither symmetric nor anti-symmetric in the vicinity of $z_{13} = 0$ and $z_{23} = 0$. This reflects the fact that the interspecies degrees of freedom of the two-component Fermi gas with $n > 2$ are not con-

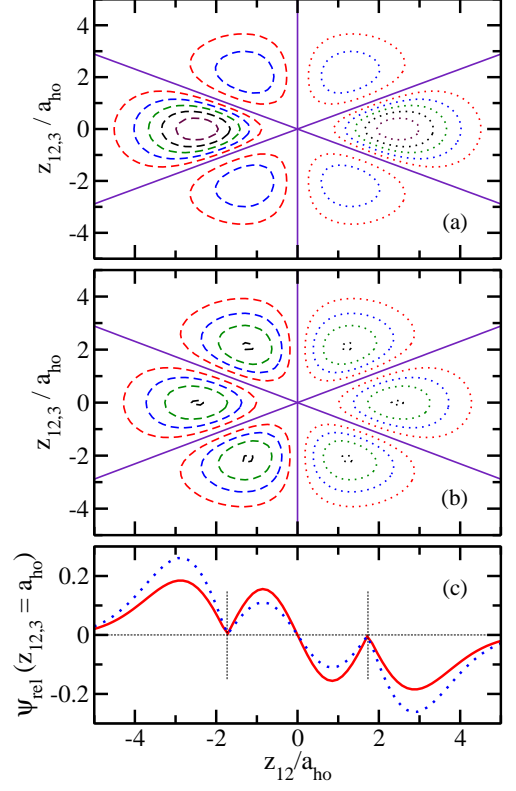


FIG. 2: (Color online) Relative wave function of the (2,1) system with $1/|g| = 0$ and $\Pi^{\text{rel}} = -1$. Contour plots of (a) $\psi_{\text{adia},1}^{|g|=\infty}$ and (b) $\psi_{G,0}$ as functions of z_{12} and $z_{12,3}$. Nodal lines are shown by solid lines. The dashed and dotted contours indicate positive and negative wave function regions; the contours are spaced equidistant. (c) Dotted and solid lines show cuts of $\psi_{\text{adia},1}^{|g|=\infty}$ and $\psi_{G,0}$ as a function of z_{12} for $z_{12,3} = a_{\text{ho}}$. The thin dashed vertical lines at $z_{12} = \pm\sqrt{3}a_{\text{ho}}$ are shown as a guide to the eye.

strained by symmetry.

Next, we discuss the correlations of the upper branch of the (2,1), (3,1) and (2,2) systems. Figure 3 shows the expectation values $\langle |z_{12}| \rangle$ and $\langle |z_{1n}| \rangle$ as a function of $-1/g$. The expectation value $\langle |z_{1n}| \rangle$ of the up-down distance coordinate increases monotonically with increasing $-1/g$ for all three systems considered. The expectation value $\langle |z_{12}| \rangle$ of the up-up distance coordinate, in contrast, first increases monotonically with increasing $-1/g$, reaches a maximum at g_c ($g_c < 0$) and then decreases monotonically. The “critical” coupling strengths are $-a_{\text{ho}}E_{\text{ho}}/g_c \approx 0.3, 0.35$ and 0.6 for the (2,1), (3,1) and (2,2) systems, respectively.

The energy of the upper branch increases monotonically with increasing $-1/g$, suggesting that the *effective* interspecies interactions for the upper branch are repulsive for all g (g positive and negative) and increase with increasing $-1/g$. In a naive picture, this suggests that the system expands with increasing $-1/g$. Indeed, this is

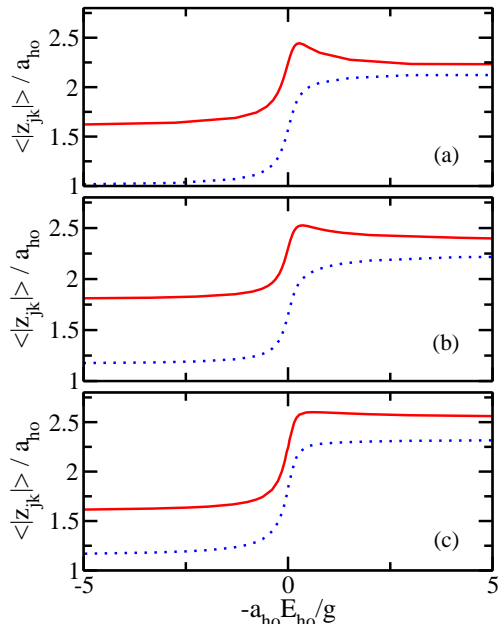


FIG. 3: (Color online) Expectation values $\langle |z_{jk}| \rangle$ for the up-up (solid lines) and up-down distance coordinate (dotted lines) as a function of $-1/g$ for the upper branches of the (a) (2, 1), (b) (3, 1), and (c) (2, 2) systems.

the case for $-1/g \lesssim -1/g_c$, as indicated by the fact that $\langle |z_{12}| \rangle$ and $\langle |z_{1n}| \rangle$ increase monotonically in this regime with increasing $-1/g$. However, $\langle |z_{12}| \rangle$ turns around at g_c , indicating that the system favors smaller distances between like particles. For $-1/g \gtrsim -1/g_c$, the interspecies interactions are so strong that they are more important than the effective repulsion due to the Pauli pressure. An analogous energy competition drives, according to the Stoner model [17], the transition from a paramagnetic phase to an itinerant ferromagnetic phase at a critical interaction strength. The metastable upper branch has been populated experimentally for small highly-elongated two-component Fermi gases [14]. These experiments suggest that decay to lower lying molecular states is negligibly small even for negative coupling

constants g , thereby opening the possibility to study the correlations discussed above experimentally.

In summary, we have solved the Schrödinger equation for harmonically confined two-component Fermi gases in one dimension as a function of the strength of the interspecies δ -function interaction. Highly accurate energy spectra were obtained for the (2, 1), (3, 1) and (2, 2) systems with positive and negative interspecies coupling constant. The strict 1d spectra agree to about 1% or better with those of quasi-1d atomic Fermi gases with aspect ratio 10 or higher [27, 36], which are currently being investigated by means of radiofrequency and tunneling spectroscopy in Jochim's cold atom laboratory in Heidelberg [13, 14]. We reported on two characteristics of the upper branch: (i) Although the energy of the upper branch coincides with that of a fully fermionized system for infinitely large coupling constant g , the corresponding eigenstate populated by adiabatically changing the system Hamiltonian does not coincide with that obtained by applying the generalized Fermi-Fermi mapping proposed in Ref. [15]. The underlying rationale is that the states of the upper branch for $n > 2$ and $n_1 - n_2 \geq 1$ are more than one-fold degenerate and that the wave function between unlike fermions is not constrained by symmetry considerations [37]. (ii) We calculated the pair-correlations of the upper branch and found that the expectation value $\langle |z_{12}| \rangle$ associated with the intraspecies distance coordinate exhibits a maximum for negative g . This, combined with the fact that the expectation value $\langle |z_{1n}| \rangle$ associated with the interspecies distance coordinate increases monotonically with increasing $-1/g$, indicates an intricate interplay between the interspecies interactions and the Pauli exclusion principle, similar to the energy competition of the Stoner model that describes the transition from paramagnetic to ferromagnetic behavior.

Note: After submission of this paper for publication, three related manuscripts appeared on the arXiv [38–40].

Acknowledgments: We acknowledge stimulating discussions and correspondence with Selim Jochim and his group members. We also acknowledge fruitful discussions with Chris H. Greene on how to connect results obtained within the Schrödinger equation and mean-field equation frameworks, and Jason Ho and Liming Guan for pointing out Ref. [16] to us. Support by the ARO is gratefully acknowledged. This work was additionally supported by the National Science Foundation through a grant for the Institute for Theoretical Atomic, Molecular and Optical Physics at Harvard University and Smithsonian Astrophysical Observatory.

-
- [1] T. Giamarchi. *Quantum Physics in One Dimension*, Oxford University Press, Oxford (2004).
 - [2] A. O. Gogolin, A. A. Nersisyan, and A. M. Tsvelik. *Bosonization and Strongly Correlated Systems*, Cam-

- bridge University Press, Cambridge, 1999.
- [3] M. A. Cazalilla, R. Citro, T. Giamarchi, E. Orignac, and M. Rigol. *Rev. Mod. Phys.* **83**, 1405 (2011).
- [4] A. Imambekov, T. L. Schmidt, and L. I. Glazman. *Rev.*

- Mod. Phys. **84**, 1253 (2012).
- [5] for a recent review, see X.-W. Guan, M. T. Batchelor, and A. Lee. arXiv:1301.6446.
 - [6] M. Girardeau. J. Math. Phys. **1**, 516 (1960).
 - [7] M. Olshanii. Phys. Rev. Lett. **81**, 938 (1998).
 - [8] P. Paredes, A. Widera, V. Murg, O. Mandel, S. Fölling, I. Cirac, G. V. Shlyapnikov, T. W. Hänsch, and I. Bloch. Nature **429**, 277 (2004).
 - [9] T. Kinoshita, T. Wenger and D. S. Weiss. Science **304**, 1125 (2004).
 - [10] T. Cheon and T. Shigehara. Phys. Lett. A **243**, 111 (1998) and Phys. Rev. Lett. **82**, 2536 (1999).
 - [11] B. E. Granger and D. Blume. Phys. Rev. Lett. **92**, 133202 (2004).
 - [12] M. D. Girardeau, H. Nguyen, and M. Olshanii. Optics Communications **243**, 3 (2004).
 - [13] G. Zürn, F. Serwane, T. Lompe, A. N. Wenz, M. G. Ries, J. E. Bohn, and S. Jochim. Phys. Rev. Lett. **108**, 075303 (2012).
 - [14] G. Zürn. *Few-fermion systems in one dimension*, Ph.D. Thesis, Ruperto-Carola-University of Heidelberg, Germany (2012).
 - [15] M. D. Girardeau. Phys. Rev. A **82**, 011607(R) (2010).
 - [16] L. Guan, S. Chen, Y. Wang, and Z.-Q. Ma. Phys. Rev. Lett. **102**, 160402 (2009).
 - [17] E. Stoner. Philos. Mag. **15**, 1018 (1933).
 - [18] G. B. Jo, Y. R. Lee, J. H. Choi, C. A. Christensen, T. H. Kim, J. H. Thywissen, D. E. Pritchard, and W. Ketterle. Science **325**, 1521 (2009).
 - [19] C. Sanner, E. J. Su, W. J. Huang, A. Keshet, J. Gillen, and W. Ketterle. Phys. Rev. Lett. **108**, 240404 (2012).
 - [20] A. Sommer, M. Ku, G. Roati, and M. W. Zwierlein. Nature **472**, 201 (2011).
 - [21] V. B. Shenoy and T.-L. Ho. Phys. Rev. Lett. **107**, 210401 (2011).
 - [22] D. Pekker, M. Babadi, R. Sensarma, N. Zinner, L. Pollet, M. W. Zwierlein, and E. Demler. Phys. Rev. Lett. **106**, 050402 (2011).
 - [23] X.-J. Liu, H. Hui, and P. D. Drummond. Phys. Rev. A **82**, 023619 (2010).
 - [24] S. Pilati, G. Bertaina, S. Giorgini, and M. Troyer. Phys. Rev. Lett. **105**, 030405 (2010).
 - [25] S.-Y. Chang, M. Randeria, and N. Trivedi. Proc. Natl. Acad. Sci. **108**, 51 (2011).
 - [26] T. Busch, B.-G. Englert, K. Rzazewski, and M. Wilkens, Found. Phys. **28**, 549 (1998).
 - [27] S. E. Gharashi, K. M. Daily, and D. Blume. Phys. Rev. A **86**, 042702 (2012).
 - [28] C. Mora, R. Egger, A. O. Gogolin, and A. Komnik, Phys. Rev. Lett. **93**, 170403 (2004).
 - [29] C. Mora, R. Egger, and A. O. Gogolin, Phys. Rev. A **71**, 052705 (2005).
 - [30] J. P. Kestner and L.-M. Duan, Phys. Rev. A **76**, 033611 (2007).
 - [31] The supplemental material at www.to.be.inserted.by.the.editor provides some technical details and tabulates the energies of the upper branch of the (2,1), (3,1) and (2,2) systems as a function of $-1/g$.
 - [32] The deviations from the expected values are within our estimated numerical uncertainties for all three systems considered.
 - [33] The construction of the adiabatic wave functions for the (2,1), (3,1) and (4,1) systems and the connection with the group theoretical analysis of Ref. [16] are presented in the supplemental material at www.to.be.inserted.by.the.editor.
 - [34] I. Brouzos and P. Schmelcher. Phys. Rev. A **87**, 023605 (2013).
 - [35] N. L. Harshman. Phys. Rev. A **86**, 052122 (2012).
 - [36] D. Blume and S. E. Gharashi, unpublished.
 - [37] As pointed out in Ref. [15], the $(n_1, n_2) = (1, 1)$ eigenstates for $1/|g| = 0$ are correctly described by the generalized Fermi-Fermi mapping. In fact, in this case, the Bose-Fermi mapping and the generalized Fermi-Fermi mapping yield the same eigenstates.
 - [38] E. J. Lindgren, J. Rotureau, C. Forssen, A. G. Volosniev, and N. T. Zinner, arXiv:1304.2992v1.
 - [39] P. O. Bugnion and G. J. Conduit, arXiv:1304.3299v1.
 - [40] T. Sowinski, T. Grass, O. Dutta, and M. Lewenstein, arXiv:1304.8099v1.

Supplemental material for “Correlations of the upper branch of 1d harmonically trapped two-component Fermi gases”

Seyed Ebrahim Gharashi¹ and D. Blume^{1,2}

¹*Department of Physics and Astronomy, Washington State University, Pullman, Washington 99164-2814, USA*

²*ITAMP, Harvard-Smithsonian Center for Astrophysics,
60 Garden Street, Cambridge, Massachusetts 02138, USA*

A. Lippmann-Schwinger equation approach

This section of the supplemental material tabulates the relative energies $E_{n_1, n_2}^{\text{rel}}$ of the upper branch of the strictly 1d harmonically trapped (2, 1), (3, 1) and (2, 2) systems. The notation and units are the same as those introduced in the main part of the paper. To solve the relative time-independent Schrödinger equation, we reformulate the problem in terms of the Lippmann-Schwinger equation and expand the relative Green’s function in terms of harmonic oscillator states (see Refs. [1–4] for details). For the three-particle system, we use the Jacobi coordinates z_{12} and $z_{12,3}$, where $z_{12,3} = (z_1 + z_2 - 2z_3)/\sqrt{3}$. For the four-particle systems, we use a set of Jacobi coordinates based on an H-tree, $z_1 - z_3$, $z_2 - z_4$ and $(z_1 + z_3 - z_2 - z_4)/\sqrt{2}$. These coordinates allow for a fairly straightforward implementation of the permutation symmetry under exchange of identical particles. Taking advantage of the fact that the two-particle Green’s function is known analytically [1, 5], the solution reduces to solving a matrix equation of infinite dimension. In practice, the matrix is truncated at dimension N_{max} . The matrix equation is most readily solved by inputting the energy. The eigenvalues of the matrix equation then yield the corresponding coupling constants g . Tables I, II and III provide the relative energies $E_{n_1, n_2}^{\text{rel}}$ of the upper branch of the (2, 1), (3, 1) and (2, 2) systems as a function of $-1/g$. The reported $-1/g$ values are found by analyzing the energy spectrum as a function of N_{max} and by extrapolating to the $N_{\text{max}} \rightarrow \infty$ limit. The largest N_{max} value considered for the (2, 1), (3, 1) and (2, 2) systems is 48, 51 and 85, respectively.

TABLE I: Relative energies of the (2, 1) system.

$-a_{\text{ho}}E_{\text{ho}}/g$	$E_{2,1}^{\text{rel}}/E_{\text{ho}}$
$-\infty$	2
−48.4533891(2)	2.0123
−5.1278666(2)	2.1123
−2.6150182(3)	2.2123
−1.7094476(3)	2.3123
−1.2415419(3)	2.4123
−0.9549028(4)	2.5123
−0.7606197(4)	2.6123
Continued on next page	

TABLE I – continued from previous page

$-a_{\text{ho}}E_{\text{ho}}/g$	$E_{2,1}^{\text{rel}}/E_{\text{ho}}$
-0.6197006(4)	2.7123
-0.5123436(4)	2.8123
-0.4274186(4)	2.9123
-0.358181(2)	3.0123
-0.300302(2)	3.1123
-0.250867(2)	3.2123
-0.207835(2)	3.3123
-0.1697307(6)	3.4123
-0.1354493(4)	3.5123
-0.1041445(4)	3.6123
-0.0751464(4)	3.7123
-0.0479103(4)	3.8123
-0.0219798(4)	3.9123
0.0030405(4)	4.0123
0.0275060(3)	4.1123
0.0517481(3)	4.2123
0.07609125(6)	4.3123
0.1008669(2)	4.4123
0.1264330(3)	4.5123
0.1531951(4)	4.6123
0.1816383(4)	4.7123
0.2123689(4)	4.8123
0.2461838(4)	4.9123
0.2841664(4)	5.0123
0.3278397(3)	5.1123
0.3796384(4)	5.2123
0.4430631(4)	5.3123
0.5242584(4)	5.4123
0.6342682(4)	5.5123
0.7954829(4)	5.6123
1.0613401(3)	5.7123
1.5990019(3)	5.8123
3.33765268(4)	5.9123
∞	6

TABLE II: Relative energies of the (3, 1) system.

$-a_{\text{ho}}E_{\text{ho}}/g$	$E_{3,1}^{\text{rel}}/E_{\text{ho}}$
$-\infty$	9/2
-60.652656(2)	4.5123
-6.497655(4)	4.6123
-3.358608(8)	4.7123
-2.22879(2)	4.8123
-1.64619(2)	4.9123
-1.29032(2)	5.0123
-1.05008(3)	5.1123
-0.87672(3)	5.2123
-0.74551(3)	5.3123
-0.64258(3)	5.4123
-0.55951(3)	5.5123
-0.49092(3)	5.6123
-0.43320(4)	5.7123
-0.38383(4)	5.8123
-0.34104(4)	5.9123
-0.30345(5)	6.0123
-0.27010(5)	6.1123
-0.24021(5)	6.2123
-0.21317(5)	6.3123
-0.18851(5)	6.4123
-0.16584(5)	6.5123
-0.14484(5)	6.6123
-0.12525(6)	6.7123
-0.10686(6)	6.8123
-0.08946(7)	6.9123
-0.07291(6)	7.0123
-0.05705(6)	7.1123
-0.04177(6)	7.2123
-0.02694(8)	7.3123
-0.01250(7)	7.4123
0.00169(6)	7.5123
0.01572(6)	7.6123
0.02964(5)	7.7123
0.04357(5)	7.8123
0.05757(5)	7.9123

Continued on next page

TABLE II – continued from previous page

$-a_{\text{ho}}E_{\text{ho}}/g$	$E_{3,1}^{\text{rel}}/E_{\text{ho}}$
0.07170(8)	8.0123
0.08612(4)	8.1123
0.10090(8)	8.2123
0.11610(8)	8.3123
0.13181(2)	8.4123
0.14824(6)	8.5123
0.16547(3)	8.6123
0.18371(2)	8.7123
0.20313(2)	8.8123
0.22401(2)	8.9123
0.24666(2)	9.0123
0.27147(3)	9.1123
0.29897(3)	9.2123
0.32990(3)	9.3123
0.36510(3)	9.4123
0.40592(3)	9.5123
0.45430(3)	9.6123
0.51307(4)	9.7123
0.58675(4)	9.8123
0.68286(3)	9.9123
0.81511(3)	10.0123
1.01124(3)	10.1123
1.33745(2)	10.2123
2.000864(8)	10.3123
4.152703(4)	10.4123
∞	21/2

TABLE III: Relative energies of the (2, 2) system.

$-a_{\text{ho}}E_{\text{ho}}/g$	$E_{2,2}^{\text{rel}}/E_{\text{ho}}$
$-\infty$	7/2
-89.000659(3)	3.5123
-9.57445(3)	3.6123
-4.97170(4)	3.7123
-3.31587(5)	3.8123
-2.46271(8)	3.9123
-1.9421(2)	4.0123

Continued on next page

TABLE III – continued from previous page

$-a_{\text{ho}}E_{\text{ho}}/g$	$E_{2,2}^{\text{rel}}/E_{\text{ho}}$
-1.5912(2)	4.1123
-1.3384(2)	4.2123
-1.1476(3)	4.3123
-0.9983(2)	4.4123
-0.8781(3)	4.5123
-0.7794(3)	4.6123
-0.6966(3)	4.7123
-0.6263(3)	4.8123
-0.5656(4)	4.9123
-0.5129(4)	5.0123
-0.4663(4)	5.1123
-0.4251(4)	5.2123
-0.3882(4)	5.3123
-0.3548(5)	5.4123
-0.3245(4)	5.5123
-0.2969(4)	5.6123
-0.2717(5)	5.7123
-0.2483(4)	5.8123
-0.2267(5)	5.9123
-0.2066(5)	6.0123
-0.1878(6)	6.1123
-0.1700(5)	6.2123
-0.1530(4)	6.3123
-0.1374(4)	6.4123
-0.1223(3)	6.5123
-0.1081(8)	6.6123
-0.0937(6)	6.7123
-0.0813(5)	6.8123
-0.0685(5)	6.9123
-0.056286(5)	7.0123
-0.0442(6)	7.1123
-0.0326(5)	7.2123
-0.0211(6)	7.3123
-0.0099(6)	7.4123
0.0012(4)	7.5123
0.0120(5)	7.6123
0.0228(5)	7.7123

Continued on next page

TABLE III – continued from previous page

$-a_{\text{ho}}E_{\text{ho}}/g$	$E_{2,2}^{\text{rel}}/E_{\text{ho}}$
0.0336(5)	7.8123
0.0444(4)	7.9123
0.0552(5)	8.0123
0.0662(5)	8.1123
0.0774(3)	8.2123
0.0887(4)	8.3123
0.0975(8)	8.4123
0.1110(5)	8.5123
0.1223(8)	8.6123
0.1354(3)	8.7123
0.1479(3)	8.8123
0.1610(3)	8.9123
0.1747(2)	9.0123
0.1909(8)	9.1123
0.20389(1)	9.2123
0.2197(2)	9.3123
0.23636(7)	9.4123
0.2540(2)	9.5123
0.2731(2)	9.6123
0.2939(2)	9.7123
0.316(2)	9.8123
0.3411(2)	9.9123
0.3684(3)	10.0123
0.3991(3)	10.1123
0.4338(3)	10.2123
0.4737(3)	10.3123
0.5202(3)	10.4123
0.5752(3)	10.5123
0.6416(4)	10.6123
0.7240(4)	10.7123
0.8295(4)	10.8123
0.9695(3)	10.9123
1.1653(3)	11.0123
1.4603(3)	11.1123
1.9575(3)	11.2123
2.9796(2)	11.3123
6.15090(2)	11.4123

Continued on next page

TABLE III – continued from previous page

$-a_{\text{ho}}E_{\text{ho}}/g$	$E_{2,2}^{\text{rel}}/E_{\text{ho}}$
∞	$23/2$

B. ψ_{adia} for $1/|g| = \infty$ for the (2, 1), (3, 1) and (2, 2) systems

This subsection discusses the construction of the adiabatic eigenfunctions of the (2, 1), (3, 1) and (2, 2) systems for infinitely large coupling constant g .

We first consider the (2, 1) system. Our calculation yields $\psi_{\text{adia},1}^{|g|=\infty}$ in numerical form. The wave function $\psi_{\text{adia},2}^{|g|=\infty}$, which corresponds to the state that is not affected by the interactions [see dashed line at $E_{2,1}^{\text{rel}} = 4E_{\text{ho}}$ in Fig. 1(a) of the main text], is known analytically. This allows us to write $\psi_{\text{G},0} = c_{\text{adia},1}\psi_{\text{adia},1}^{|g|=\infty} + c_{\text{adia},2}\psi_{\text{adia},2}^{|g|=\infty}$, where $c_{\text{adia},2}$ can be found analytically and $c_{\text{adia},1}$ can be obtained numerically by calculating the overlap between $\psi_{\text{adia},1}^{|g|=\infty}$ (known in numerical form) and $\psi_{\text{G},0}$. Plugging $|c_{\text{adia},2}|^2 = 1/9$ into $|c_{\text{adia},1}|^2 + |c_{\text{adia},2}|^2 = 1$, we find $|c_{\text{adia},1}|^2 = 8/9 \approx 0.888888$. For comparison, our numerically determined value is $|c_{\text{adia},1}|^2 = 0.888886(2)$. Lastly, using $\psi_{\text{adia},1}^{|g|=\infty} = (\psi_{\text{G},0} - c_{\text{adia},2}\psi_{\text{adia},2}^{|g|=\infty})/c_{\text{adia},1}$, we find the analytical expression given in Eq. (2) of the main text. The analytical wave functions deduced from our numerical approach agree with those obtained via a group theoretical approach. Application of Eqs. (4) and (5) of Ref. [6] yields $\psi_{\text{adia},1}^{|g|=\infty}$ [in fact, it yields a linear combination of three wave functions, where the spin-up and spin-down particles are ordered up-up-down (the labeling chosen in the present work), up-down-up and down-up-up]. In the language of Ref. [6], $\psi_{\text{adia},2}^{|g|=\infty}$ is associated with a ferromagnetic spin state and given by Eq. (3) of Ref. [6]. For completeness, we also report the normalized adiabatic (2, 1) wave function with even parity for $1/|g| = 0$,

$$\frac{a_{\text{ho}}^{-9/2}}{2\pi^{3/4}} z_{12} \left(|z_{13}| z_{23} + z_{13} |z_{23}| \right) f(z_1, z_2, z_3). \quad (1)$$

While the group theoretical approach of Ref. [6] directly yields the adiabatic eigenstates $\psi_{\text{adia},1}^{|g|=\infty}$ and $\psi_{\text{adia},2}^{|g|=\infty}$ for the (2, 1) systems, this is *not* the case for the (3, 1) and (2, 2) systems. For the (3, 1) system, e.g., application of Eqs. (4) and (5) of Ref. [6] yields $\psi_{\text{G},0}$. To obtain the adiabatic eigenstates of the (3, 1) and (2, 2) systems, appropriate linear combinations of the states constructed using the approach of Ref. [6] have to be taken. In the following, we report the adiabatic eigenstates of the energetically lowest-lying degenerate (3, 1) and (2, 2) energy manifolds for $1/|g| = 0$.

For the (3, 1) system, the normalized adiabatic eigenstates with odd parity read

$$\psi_{\text{adia},1}^{|g|=\infty} = \frac{a_{\text{ho}}^{-8}}{3\pi\sqrt{10}} z_{12} z_{13} z_{23} \left(|z_{14}| z_{24} z_{34} + z_{14} |z_{24}| z_{34} + z_{14} z_{24} |z_{34}| - 5|z_{14}| |z_{24}| |z_{34}| \right) f(z_1, z_2, z_3, z_4) \quad (2)$$

and

$$\psi_{\text{adia},2}^{|g|=\infty} = \frac{\sqrt{2}a_{\text{ho}}^{-8}}{3\pi\sqrt{5}} z_{12} z_{13} z_{23} \left(|z_{14}| z_{24} z_{34} + z_{14} |z_{24}| z_{34} + z_{14} z_{24} |z_{34}| \right) f(z_1, z_2, z_3, z_4). \quad (3)$$

We find $|\langle \psi_{\text{adia},j}^{|g|=\infty} | \psi_{\text{G},0} \rangle|^2 = 4/5$ and $1/5$ for $j = 1$ and 2 , respectively. For completeness, we also report the adiabatic eigenstates of the two even parity states,

$$\frac{a_{\text{ho}}^{-8}}{3\pi\sqrt{2}} z_{12} z_{13} z_{23} \left(z_{14} z_{24} z_{34} - |z_{14}| |z_{24}| z_{34} - |z_{14}| z_{24} |z_{34}| - z_{14} |z_{24}| |z_{34}| \right) f(z_1, z_2, z_3, z_4) \quad (4)$$

and

$$\psi_{\text{ideal},0} = \frac{\sqrt{2}a_{\text{ho}}^{-8}}{3\pi} z_{12} z_{13} z_{14} z_{23} z_{24} z_{34} f(z_1, z_2, z_3, z_4). \quad (5)$$

For the (2, 2) system, the normalized adiabatic eigenstates with even parity read

$$\begin{aligned} \psi_{\text{adia},1}^{|g|=\infty} = & \frac{a_{\text{ho}}^{-8}}{12\sqrt{13}\pi} z_{12} z_{34} \left\{ \left[-8c_0 - 3\sqrt{3}(1 - c_0^2)^{1/2} \right] z_{13} z_{14} z_{23} z_{24} + \right. \\ & \left[6c_0 - \sqrt{3}(1 - c_0^2)^{1/2} \right] \left(|z_{13}| |z_{14}| z_{23} z_{24} + |z_{13}| z_{14} |z_{23}| z_{24} + \right. \\ & \left. |z_{13}| z_{14} z_{23} |z_{24}| + z_{13} |z_{14}| |z_{23}| z_{24} + z_{13} |z_{14}| z_{23} |z_{24}| + z_{13} z_{14} |z_{23}| |z_{24}| \right) \\ & \left. + 13\sqrt{3}(1 - c_0^2)^{1/2} |z_{13}| |z_{14}| |z_{23}| |z_{24}| \right\} f(z_1, z_2, z_3, z_4), \end{aligned} \quad (6)$$

$$\begin{aligned} \psi_{\text{adia},2}^{|g|=\infty} = & \frac{a_{\text{ho}}^{-8}}{2\sqrt{6}\pi} z_{12} z_{34} \left(|z_{13}| |z_{14}| z_{23} z_{24} - z_{13} |z_{14}| z_{23} |z_{24}| - \right. \\ & \left. |z_{13}| z_{14} |z_{23}| z_{24} + z_{13} z_{14} |z_{23}| |z_{24}| \right) f(z_1, z_2, z_3, z_4), \end{aligned} \quad (7)$$

$$\begin{aligned} \psi_{\text{adia},3}^{|g|=\infty} = & \frac{a_{\text{ho}}^{-8}}{12\sqrt{13}\pi} z_{12} z_{34} \left\{ \left[3\sqrt{3}c_0 - 8(1 - c_0^2)^{1/2} \right] z_{13} z_{14} z_{23} z_{24} + \right. \\ & \left[\sqrt{3}c_0 + 6(1 - c_0^2)^{1/2} \right] \left(|z_{13}| |z_{14}| z_{23} z_{24} + |z_{13}| z_{14} |z_{23}| z_{24} + |z_{13}| z_{14} z_{23} |z_{24}| + \right. \\ & \left. z_{13} |z_{14}| |z_{23}| z_{24} + z_{13} |z_{14}| z_{23} |z_{24}| + z_{13} z_{14} |z_{23}| |z_{24}| \right) \\ & \left. - 13\sqrt{3}c_0 |z_{13}| |z_{14}| |z_{23}| |z_{24}| \right\} f(z_1, z_2, z_3, z_4) \end{aligned} \quad (8)$$

and

$$\psi_{\text{adia},4}^{|g|=\infty} = \psi_{\text{ideal},0}. \quad (9)$$

Here,

$$c_0 = \sqrt{1 - \frac{\left(3\sqrt{6}c + 2\sqrt{1 - 9c^2/8} \right)^2}{52}} \quad (10)$$

with $c = |\langle \psi_{\text{adia},1}^{|g|=\infty} | \psi_{\text{G},0} \rangle|$ is determined numerically. We find $|\langle \psi_{\text{adia},j}^{|g|=\infty} | \psi_{\text{G},0} \rangle|^2 \approx 0.865(7)$, 0, 0.023(6) and 1/9 for $j = 1, 2, 3$ and 4, respectively. For completeness, we also report the adiabatic eigenstates of the two odd parity states,

$$\frac{a_{\text{ho}}^{-8}}{\sqrt{30}\pi} z_{12} z_{34} \left(|z_{13}| z_{14} z_{23} z_{24} + z_{13} |z_{14}| z_{23} z_{24} + z_{13} z_{14} |z_{23}| z_{24} + z_{13} z_{14} z_{23} |z_{24}| \right) f(z_1, z_2, z_3, z_4) \quad (11)$$

and

$$\frac{a_{\text{ho}}^{-8}}{4\sqrt{30}\pi} z_{12} z_{34} \left(-3 |z_{13}| z_{14} z_{23} z_{24} - 3 z_{13} |z_{14}| z_{23} z_{24} - 3 z_{13} z_{14} |z_{23}| z_{24} - 3 z_{13} z_{14} z_{23} |z_{24}| + \right. \\ \left. 5 z_{13} |z_{14}| |z_{23}| |z_{24}| + 5 |z_{13}| z_{14} |z_{23}| |z_{24}| + 5 |z_{13}| |z_{14}| z_{23} |z_{24}| + 5 |z_{13}| |z_{14}| |z_{23}| z_{24} \right) f(z_1, z_2, z_3, z_4). \quad (12)$$

-
- [1] S. E. Gharashi, K. M. Daily, and D. Blume. Phys. Rev. A **86**, 042702 (2012).
 - [2] C. Mora, R. Egger, A. O. Gogolin, and A. Komnik. Phys. Rev. Lett. **93**, 170403 (2004).
 - [3] C. Mora, R. Egger, and A. O. Gogolin. Phys. Rev. A **71**, 052705 (2005).
 - [4] J. P. Kestner and L.-M. Duan. Phys. Rev. A **76**, 033611 (2007).
 - [5] T. Busch, B.-G. Englert, K. Rzażewski, and M. Wilkens. Found. Phys. **28**, 549 (1998).
 - [6] L. Guan, S. Chen, Y. Wang, and Z.-Q. Ma. Phys. Rev. Lett. **102**, 160402 (2009).